

Sara DUDZIŃSKA, Emilia BACHTIAK-RADKA, Daniel GROCHAŁA, Stefan BERCZYŃSKI

West Pomeranian University of Technology, Szczecin, Poland
Department of Mechanical Engineering and Mechatronics
emilia.bachtiak-radka@zut.edu.pl; daniel.grochala@zut.edu.pl

A STUDY ON TECHNOLOGICAL PROPERTIES OF METALLIC SURFACES MARKED WITH DATA MATRIX CODES WITH LASER TECHNOLOGY

© 2018 Sara Dudzińska, Emilia Bachtiak-Radka, Daniel Grochala, Stefan Berczyński

This is an open access article licensed under the Creative Commons Attribution International License (CC BY)



<https://creativecommons.org/licenses/by/4.0/>

Key words: Data Matrix codes, laser technology, metallic surfaces, chromatic confocal probe, surface topography measurements.

Abstract: Marking products manufactured from steel and non-ferrous metals is a very important part of the process. Generally, they are used in the production of parts responsible for the health and safety of people in the airline, automotive, and machine industries. The tessellated code is usually applied on the surfaces by laser techniques in the initial phase of the process. A shaping method of the surface that contains the encoded data of the dimensions and used technology must be readable despite subsequent treatment. The surface of the code must be resistant to mechanical damage, further processing, and electrolytic corrosion. The article will present the test results for aluminium surfaces marked by laser; wherein, as a result of a subsequent electrolytic treatment, a different class code and the contrast between pixels were acquired.

Badanie właściwości technologicznych powierzchni metalowych oznaczonych kodami Data Matrix w technologii laserowej

Słowa kluczowe: Data Matrix kody, technologia laserowa, powierzchnie metalowe, chromatyczna sonda konfokalna, pomiary topografii powierzchni.

Streszczenie: Znakowanie produktów wykonanych ze stali i metali nieżelaznych jest bardzo ważną częścią procesu. Kodowania danych są wykorzystywane po produkcji części odpowiedzialnych za zdrowie i bezpieczeństwo ludzi w branży lotniczej, motoryzacyjnej i maszynowej. Mozaikowy kod jest zwykle nałożony na powierzchnie za pomocą technik laserowych w początkowej fazie procesu. Sposób oznaczania powierzchni, która zawiera zakodowane dane procesowe oraz technologia oznaczania wyrobu muszą zapewniać możliwość odczytywania tych informacji pomimo dalszego przetwarzania. Powierzchnia kodu musi być odporna na uszkodzenia mechaniczne, dalszą obróbkę i korozję elektrolityczną. W artykule zostaną przedstawione wyniki badań dla powierzchni aluminiowych oznaczonych laserem, w których w następstwie obróbki elektrolitycznej następowała utrata jakości kodu i kontrast pomiędzy pikselami.

Introduction

Information flow plays an important role in everyday life, mass media, and industry. After initial processing, new information should be recorded unambiguously with a standard enabling further processing. Information recording, its further processing, distribution, and protection are all features that have allowed human beings to develop civilisation.

Information that is recorded can be later shared. The choice of information carrier determines data

durability, retrieval, and processing. Problems of data storage may arise due to unsatisfactory carrier capability (a sheet of paper, a CD, a 64GB pendrive). However, the capability can be increased by changing one carrier into another. A carrier change causes another problem of the ease of data access. A sheet of paper can be read without any equipment but CDs or flash memory discs need a computer. A similar problem arises in data recording.

It is useful, therefore, to have a data recording format which can store many signs in a small space without having to miniaturise symbol size. 2D Data

Matrix codes provide an opportunity [1–3]. They can use almost any material as a carrier, which can change light properties depending on the angle of incidence. The resultant contrast in different areas (colour change, brightness) determines differences between signs. An appropriate coding system can reduce the number of symbols and increase data storage capability [3, 4]. Recently, 2D Data Matrix codes have come into common use. They can be embedded on the surface of many different materials. Two signs only, 0/1, are required for binary coding. Pixels are usually used as symbols [1–4]. They must be regular and easy to read for automatic decoding systems. Code readability loss may arise from contrast loss between pixels. Code readability loss results in irrevocable loss of information.

This paper presents experimental results of code durability and readability. Codes were embedded on the surface of objects made of cast aluminium alloys using various laser techniques of pixel embedding. Code durability also depended on technological parameters of further processes.

1. Product marking with 2D QR codes

2D Data Matrix codes are commonly used in information flow, and their use is predicted to grow further and become more widespread [5]. Information is coded, it is easy to read, and coding methods provide protection for confidential data from unauthorised access [5]. Data coding is used in many areas of human activity. Links to web sites used in private life or for tourism are coded [7]. Coded data are used by corporations and administration [7]. Coding technology is used for storing information about product inspections, dimensions, and tools used for their production. Product marking is a major requirement in aviation and automotive industries which use products responsible for human health and safety – Fig. 1.

Self-adhesive stickers are printed and printing techniques are used for embedding codes directly on a rough product surface. Laser and mechanical marking methods of products are also in common use. Standards such as Data Matrix, DataBar, and QR are used in product

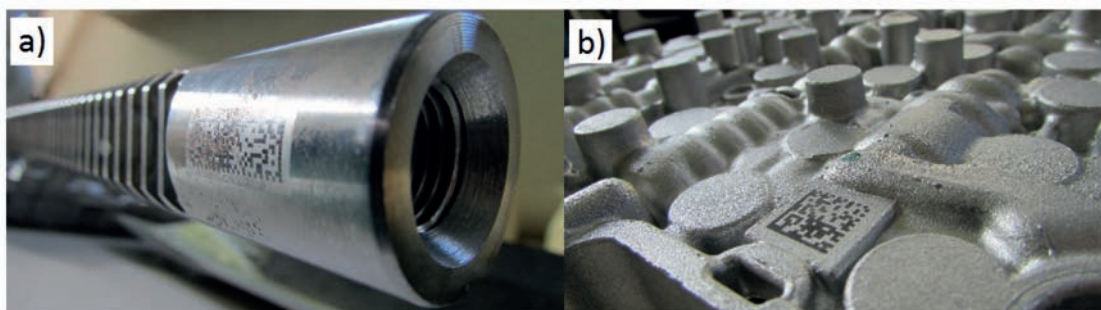


Fig. 1. QR codes embedded with laser technique on the surface of (a) a steel part (of steering gear), (b) a logic valve aluminium housing (automatic gear box)

marking. Requirements of binary product marking are described elsewhere [1–3]. Global Language of Business GS1 requirements define areas where coded marking is embedded onto products and technical requirements of a code.

Error avoidance is important during code embedding, because errors may inhibit data access. Methods and requirements of error correction and code validation are presented in norm definitions [1, 2]. The most common errors are presented in Fig. 2.

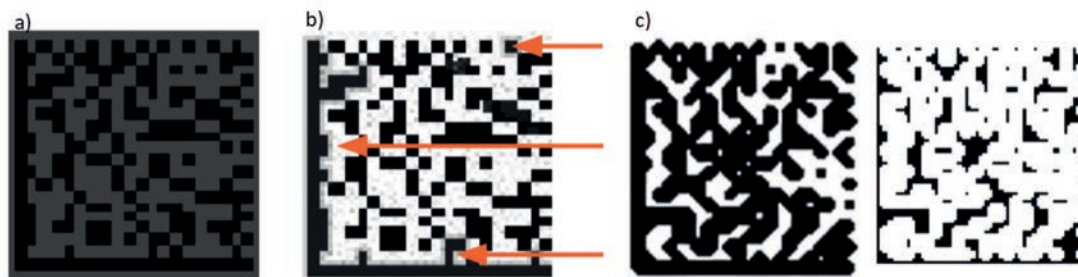


Fig. 2. Common errors of 2D QR codes [2]: a) no contrast between pixels; b) modulation – no contrast between code fragments; c) print width

Source: [2].

In manufacturing processes in aviation and automotive industries, prefabricated elements undergo initial control and then are permanently marked, which is tantamount to permission for further processing – Fig. 1b. Available marking areas are not further processed and can be easily accessed. It protects codes from mechanical damage in further processing, assembly, and operation.

Products marked according to class requirements (A or B usually – see Table 1) are further processed. Problems arise when a product made according to specification is marked as Class C or D and when, for

technological reasons, another marking is impossible. In order not to generate high rejection rate costs, high resolutions optical systems should be used for product tracking. Code data analysis needs implementation of algorithms to read very noisy signals. The smaller the code matrix, the larger the problem may be. Small matrix codes have smaller correction data redundancy.

Recently, 2D Data Matrix codes have been developed where colour is an additional information carrier [10]. For technical reasons, such codes are not currently used in industry for permanent marking of metallic parts.

Table 1. 2D Code standards – ANSI/ISO quality parameters

Short	Parameter Name	Parameter Description	Quality class of code				
			A	B	C	D	F
UEC	Unused Error Correction	This is the percentage of error correction capability that is available for further incorrect modules. The assignment of grade is as follows: UEC % Grade	62 \geq UEC	62> UEC ≥ 50	50> UEC ≥ 37	37> UEC ≥ 25	UEC < 25
SC	Symbol Contrast	This is the difference in reflectivity between the brightest module and the darkest module. The assignment of grade is as follows: SC Grade	70 \geq SC	70> SC ≥ 55	55> SC ≥ 40	40> SC ≥ 20	SC < 20
MOD	Modulation	This is a grade based on the amount of variability in reflectivity of the modules. A multi-step process is used to get the modulation grade. First the reflectivity of each module is compared to the global threshold and the overall Symbol Contrast according to the following formula: $MOD = 2 * (abs(RGT)) / SC$. The Global Threshold GT is the midpoint between the reflectance of the brightest module and the reflectance of the darkest module. Next, the grade level for each module is determined from the MOD value according to the following table: MOD % Grade. Finally, the value of the grade for the MOD parameter will be the highest modulation level for which the modules meeting that level will result in an Unused Error Correction grade of that level or higher. Note that a module which is decoded in error can still yield a high MOD value, and therefore is more related to printing contrast than RM.	60 \geq MOD	60> MOD > 40	50> MOD > 30	50> MOD > 20	MOD < 20
RM	Reflectance Margin	Is the same as Modulation, except that when a module is decoded in error (a bar whose reflectivity is higher than GT, or a space whose reflectivity is less than GT), MOD is set to 0, and therefore considered an F. RM will always be equal or lower than MOD and is more related to readability than is MOD.					
ANU	Axial Non-uniformity	This is the amount of out of square a symbol is, or in other words a measure of the overall aspect ratio of the symbol.					
GNU	Grid Non-uniformity	This is the worst case distance between the calculated center of a module and the ideal location for the center of the module based on perfectly evenly spaced modules. The calculated center of the module is determined using the clock tracks. The value is reported as a percentage of a module size.					
FPD	Finder Pattern Damage	This is the grade for all the finder pattern which is the lowest of all the following grades.					

2. Laser surface marking of metallic objects

Permanent labelling of Data Matrix codes of the workpieces from aluminium and steel is possible by the creating of a monochromatic matrix of the pixels on the surface that will be much darker than the background with a metallic gloss. Light reflectance changes translate into level of intensity. Dark pixels are where light

optics phenomena play the most important role, such as light diffraction on periodic micro-roughness on the surface [11, 12] – Fig. 3.

Pixel size depends on the size of the matrix and the code size, which is defined in norm requirements [1–2]. Errors, such as reflectance margin (MR), axial non-uniformity (ANU), grid non-uniformity (GNU), and finder pattern damage (FPD), are caused by steering errors of a laser beam onto a surface or its non-parallel positioning against the laser focus surface. Shape and

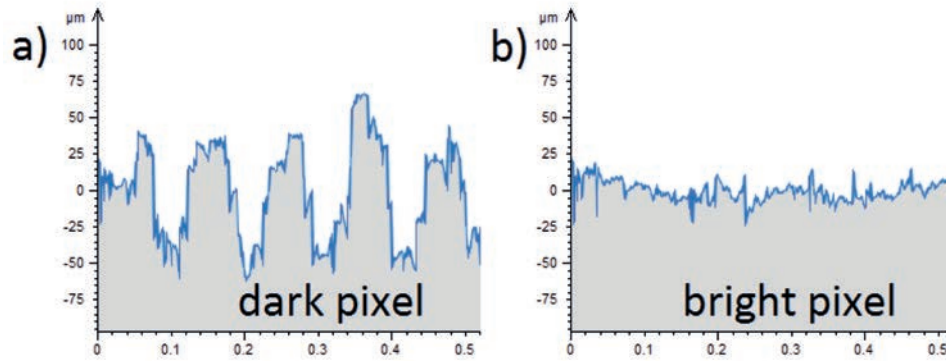


Fig. 3. A 2D code surface; a) dark pixel with average roughness height of 77 μm ; b) bright pixel with average roughness height of 12.5 μm

Source: [11, 12].

positioning errors of a part undergoing marking may also be responsible for the errors. The causes of such errors are easy to diagnose and correct.

SC and MOD errors are more difficult to correct. They are dependent on the height and regularity of deliberate surface roughness in dark pixels and areas where roughness is smoothed in bright pixels.

A laser type's (Nd-Yag, CW) power and maximum surface energy density affect the method of embedding dark and light pixels in a code. Manufacturers of laser

heads used for code embedding give the user only some parameters that control contrast and modulation. The laser mode of operation is determined by the material selected by the user [12]. Further optimisation of code quality, depending on changing production conditions, is very difficult. Contrast enhancement usually requires an increase of laser beam energy density in dark pixels. As a result, surface roughness becomes deeper without changing its number to width ratio. A Data Matrix Class A code and a scan of its pixels are shown in Fig. 4.

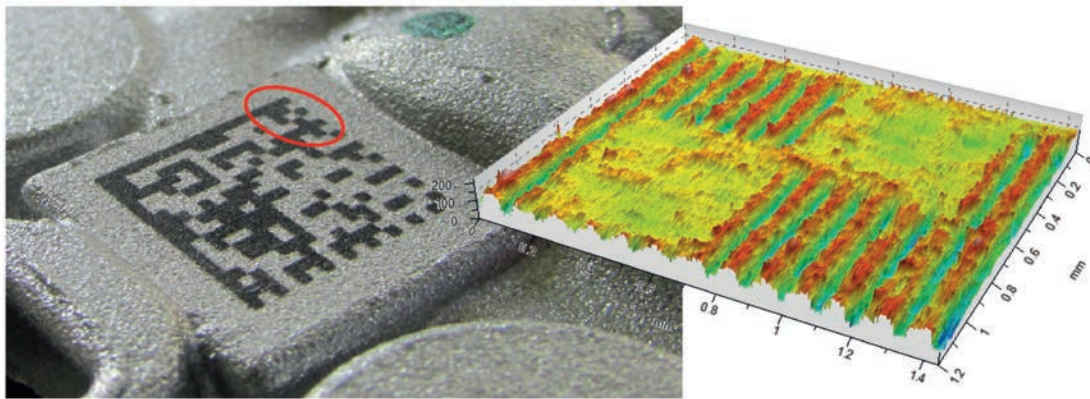


Fig. 4. A Data Matrix Class A code on an aluminium object made with Nd-Yag laser, and a scan of pixel topography

Source: Authors.

3. Effect of laser marking on code contrast and topography changes

In the Surface Topography Laboratory of West Pomeranian University of Technology, Szczecin, a study into the effect of marking method on code surface contrast and topography was conducted. The study was commissioned by an automotive company which marked its parts at the beginning of a technological

process with 2D Data Matrix codes. Class A codes suffered a substantial quality loss after completion of a technological process – Fig. 5.

In extreme cases, data access failure was signalled in final control. These parts could not be marked again. Nor could they be used for the assembly phase. The loss of code readability resulted in heavy losses generated by the company despite strict adherence to technical specifications (dimension and shape errors).



Fig. 5. Technological process of an aluminium part marked with Nd-Yag laser

Source: Authors.

Chrome rinsing treatment was the principal cause of code readability loss. The process involved electrolyte surface treatment and pixel etching. A marked decrease of SC contrast symbol was observed after treatment – Fig. 6.

Examined elements were made of an AlSiCu (EN AC-47100) alloy. Its chemical composition is presented in Table 2.

A GS1 Data Matrix square code was used for marking elements. Its technical parameters are shown in Table 3 and its pixel size was 0.5x 0.5 mm.

The aim of the study was to compare two different strategies of laser operation while marking and to evaluate which strategy turned out to be better for marking parts undergoing chrome rinse at the end of technological process – Fig. 7.

Six parts (three for each variant) were delivered for the study – Fig. 7. Markings were verified for the first time during the first control. The initial quality A was achieved for each part. Then, markings were scanned, the elements were returned, and technological operations were performed in standard conditions. Finally, the code surface was verified again, and its topography was scanned.

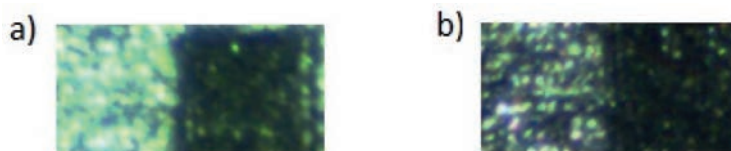


Fig. 6. Code contrast loss, A view in constant exposition conditions at 10x magnification; a) surface marked with Class A code; b) surface after chrome rinse – Class C code

Source: Authors.

Table 2. Chemical composition of aluminium alloy DIN EN 1706:2013-12

Alloy	Chemical composition [%]												
	Al	Si	Fe	Cu	Mn	Mg	Cr	Ni	Zn	Pb	Sn	Ti	Other
EN AC-47100	81.4-88.8	10.5-13.5	1.3	0.7-1.2	0.55	0.32	0.1	0.3	0.55	0.2	0.1	0.2	0.25

Table 3. The Data Matrix Symbol Attributes [2]

Symbol size		Data region		Mapping matrix size	Total code words		Maximum data capacity		% of code words used for error correction No.	Max. Correctable code words error/ erasure
Row	Col	Size	No.		Data	Error	Num. Cap.	Alpha-num. Cap.		
18	18	16x16	1	16x16	18	14	36	25	43.8	7/11

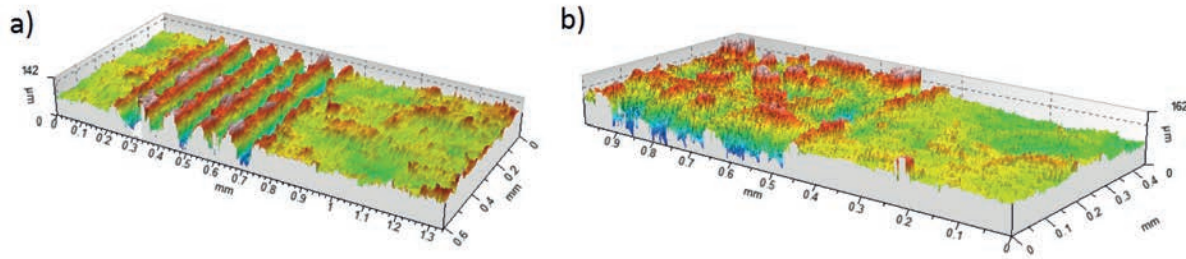


Fig. 7. A part of code surface marked with laser: a) each dark pixel made up of 6 rows, b) each dark pixel made up of 13 rows
Source: Authors.

4. Measurement methodology

SG measurements were conducted with an AltiSurf A520 multisensor, manufactured by Altimet. It was fitted with a CL1 chromatic confocal sensor [14], with a range to 130 μm and vertical resolution of 8 nm. Measurements were conducted on 2 x 2 mm areas. Experimentally determined scanning resolutions along X and Y axes were 0.068 μm and 3 μm , respectively, which generated a cloud of 19.7 mln points. Each area scan lasted almost 15 h. AltiMap PREMIUM 6.2 was used to analyse data and determine surface topography (complying with ISO 25178).

For each recorded surface point cloud, surface topography analysis involved the following:

- Cutting out three dark and three bright pixels (0.5x 0.5 mm) in 2 x 2 mm areas, for each sample (scan), six measuring areas were obtained;
- The determination of the threshold level in every cut-out area of 0.01–99.9% to delete unreliable surface data (deleted points were set as unmeasured parameters);
- Surface levelling (with mean area determined using the least square method (LS)); and,
- The determination of some stereometric roughness parameters in compliance with ISO 25178.

The mean values of recorded SG parameters are presented in Table 4.

Table 4. SG parameters

Name	Parameter description	unit	Strategy 6				Strategy 13			
			Dark pixel quality		Bright pixel quality		Dark pixel quality		Bright pixel Quality	
			A	C	A	C	A	C	A	C
Sq	Root mean square height	μm	42.695	36.188	9.444	8.032	30.329	28.669	8.417	9.424
Sz	Maximum height	μm	196.065	165.083	76.752	67.498	187.099	163.073	79.294	90.722
Sa	Arithmetical mean height	μm	37.996	31.834	7.532	6.329	24.487	23.635	6.491	7.253
Vm	Material volume	mm^3/mm^2	0.001	0.001	0.000	0.000	0.001	0.001	0.000	0.001
Vv	Void volume	mm^3/mm^2	0.052	0.044	0.013	0.010	0.038	0.035	0.011	0.012
Vmp	Peak material volume of the scale limited surface	mm^3/mm^2	0.0010	0.0008	0.0005	0.0003	0.0011	0.0008	0.0004	0.0005
Vmc	Core material volume of the scale limited surface	mm^3/mm^2	0.045	0.041	0.008	0.007	0.029	0.030	0.007	0.008
Vvc	Core void volume of the scale limited surface	mm^3/mm^2	0.050	0.042	0.012	0.009	0.034	0.031	0.010	0.011
Vvv	Pit void volume of the scale limited surface	mm^3/mm^2	0.003	0.003	0.001	0.001	0.004	0.003	0.001	0.001

5. Measurement results

Figure 8 presents surface roughness values of the Sz parameter recorded separately for dark and bright pixels. In each case, a code surface which at first was assessed as Class A was ranked as Class C after chromium rinse. Roughness height of dark pixel areas compared to that of bright pixels was, on average, 60% higher for the first laser method. In the second laser method, roughness height of dark pixel areas compared to that of bright pixels was, on average, 55% higher.

Samples provided for tests were homogeneous, which was confirmed by a small spread of observed values around the determined average figure.

After the chrome rinse, the roughness height of dark pixels (code C) decreased by approximately 15% compared to initial values (code A). Similar conclusions could not be drawn for bright pixels, since their average differences compared to the range were very small.

Height loss, i.e. the loss of contrast between dark and light pixels, was greater for the second strategy with 6 laser-made stripes, and the difference for dark pixels exceeded 30% – Fig. 9. For the first strategy, a decrease of Sz parameter change between dark and light pixels was smaller (20%).

Patterns of other SG parameters compared to those of Sz are very similar. In all cases, the functional parameters of surface area marked with laser using the first strategy significantly decreased.

Substantial changes of material volume Vm and void volume Vv are caused by major modification of dark pixel area (chrome rinse). Large differences are to be found in peak material volume Vmp, core material volume Vmc (Fig. 10), and core void volume Vvc. Changes of functional volume parameters marked with a laser using the second strategy (13 stripes) are small and within the spread.

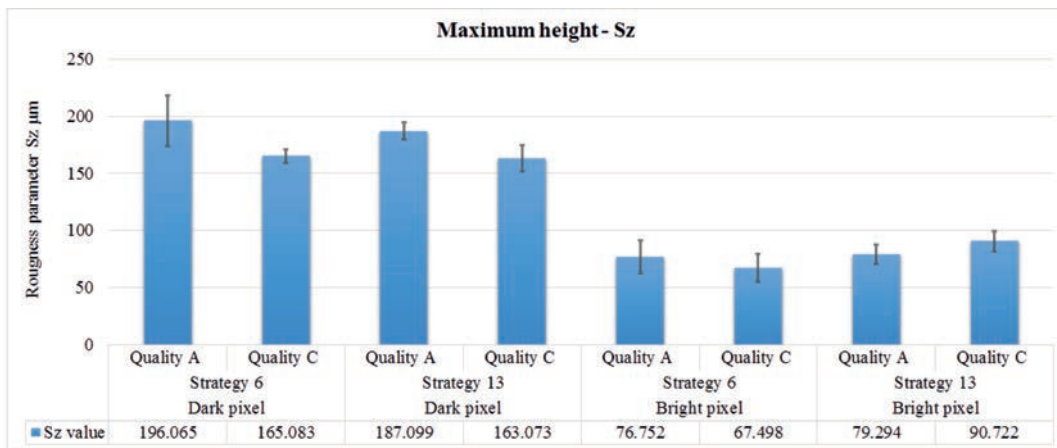


Fig. 8. Roughness results for parameter Sz obtained in the study
Source: Authors.

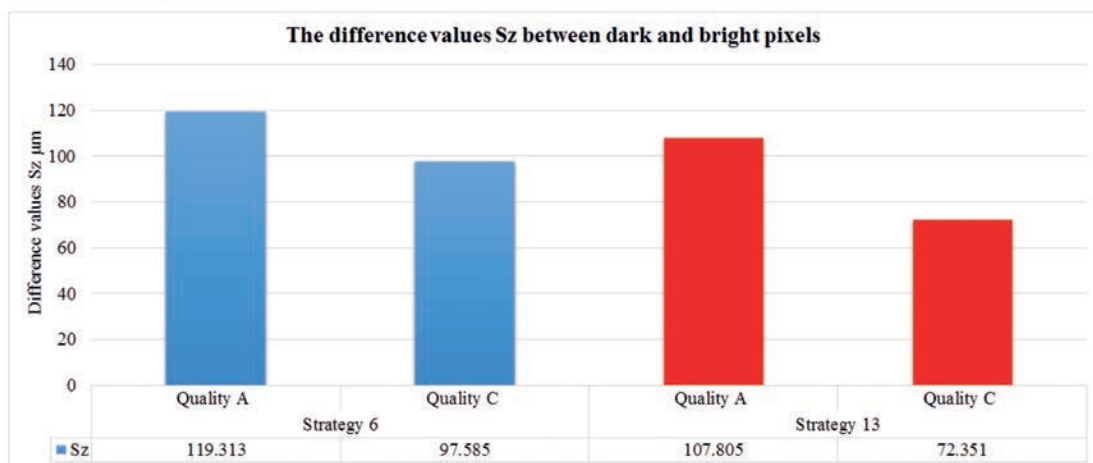


Fig. 9. Decrease of the Sz parameter between dark and light pixels after chrome rinse
Source: Authors.

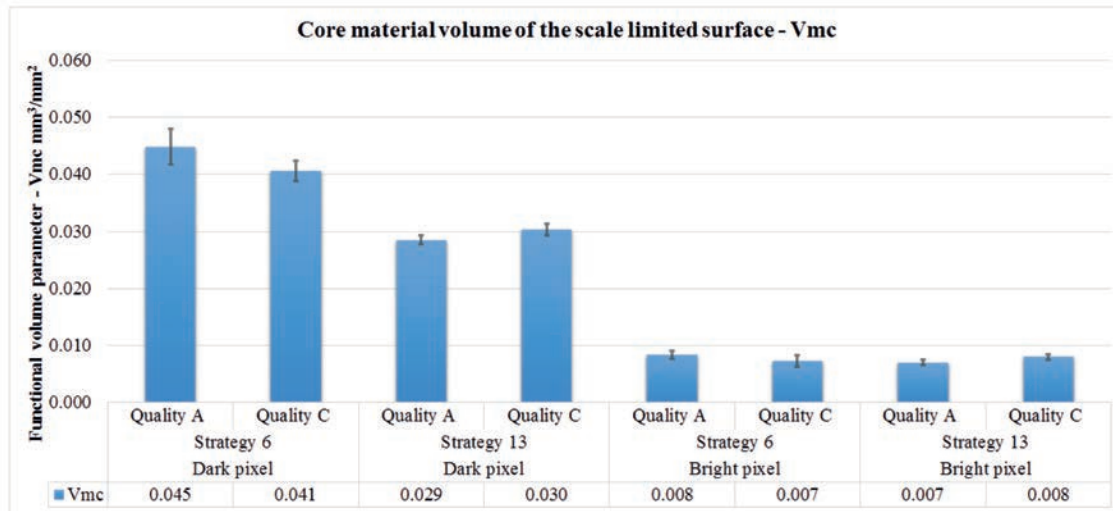


Fig. 10. Experimental values of core material volume Vmc
Source: Authors.

Differences of core material volume Vmc between bright and dark pixels were 80% for the first strategy and 75% for the other one (13 stripes on the area of a dark pixel).

Vmc values decreased by approximately 10% for the code area after chrome rinse for the first strategy. Changes of functional volume parameters marked with a laser using the second strategy (13 stripes) are small and within the spread – Fig. 11.

To maintain code contrast, dark pixel markings should have the appropriate depth (pit void volume). The diffraction of a light wave will occur on them. Pit void volume Vvv (Fig. 12) describes the void space in markings.

The biggest differences of pit void volume Vvv were observed for the second strategy of laser marking (differences for dark and bright pixels of 75%). Differences for the first strategy were only 60%.

The decrease of Vvv between dark and bright pixels due to chrome rinse was greater in the second strategy.

However, differences between Vvv of codes A and C were approximately 25%. The decrease of Vvv between dark and bright pixels in the first strategy was smaller. No significant changes between Class A and Class C codes were observed.

The decrease of roughness height SG parameters (Sq, Sz, and Sa) for dark pixels in the first strategy between Class A and Class C codes was relatively large. It demonstrated that the surface character changed, including roughness, shape, and height. Surface character was easy to change in successive treatments.

The character of observed changes was similar in the second laser strategy, involving roughness shape and height changes. However, a larger quantitative effect of the phenomena was necessary for a signal to downgrade its category from Class A to Class C. It confirmed the better resistance of the surface to chrome rinse and mechanical damage. Surface types obtained in the study are presented in Fig. 14.

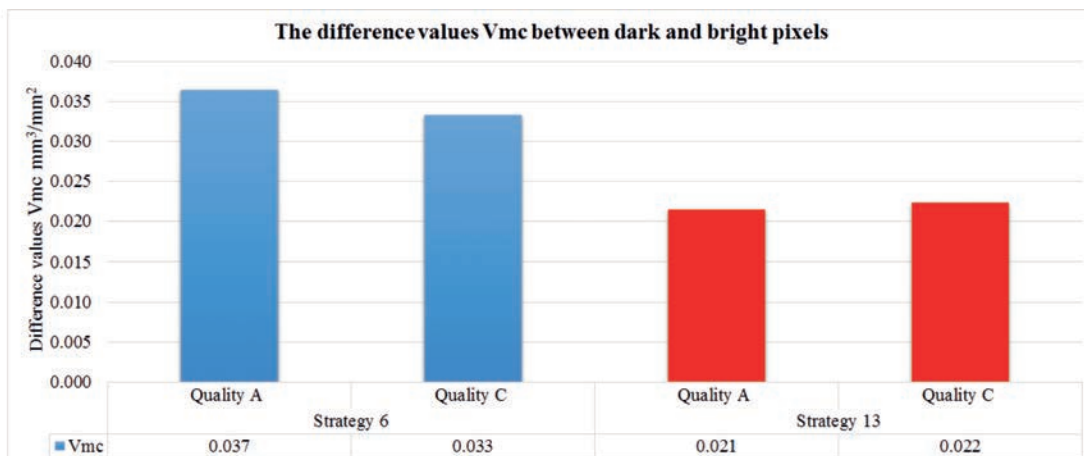


Fig. 11. Decrease of the Vmc between dark and light pixels after chrome rinse
Source: Authors.

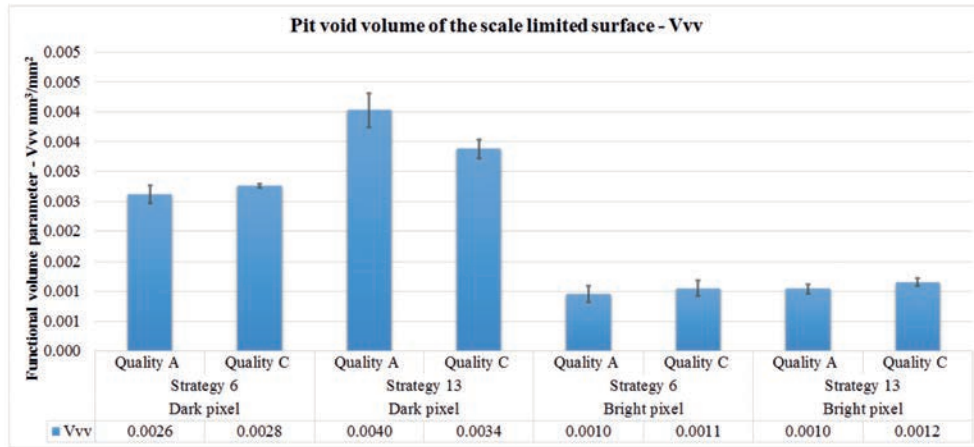


Fig. 12. Experimental values of pit void volume Vvv
Source: Authors.

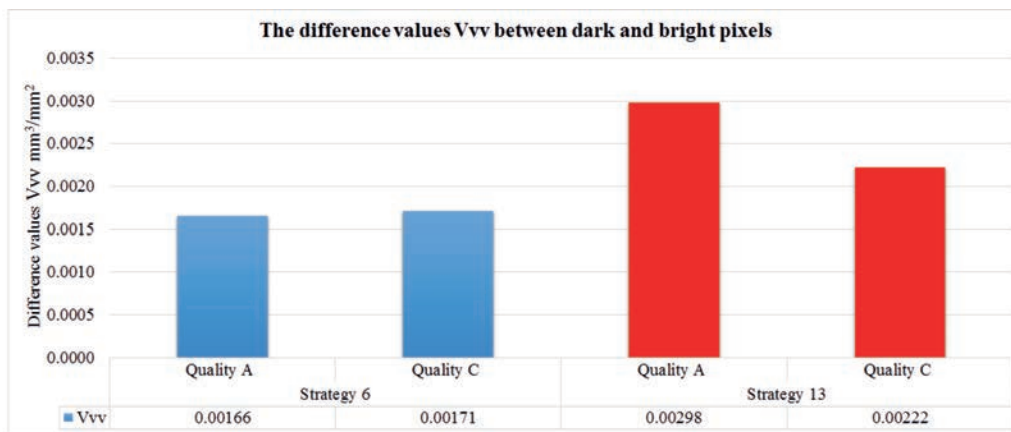


Fig. 13. Decrease of Vvv between dark and bright pixels after chrome rinse
Source: Authors.

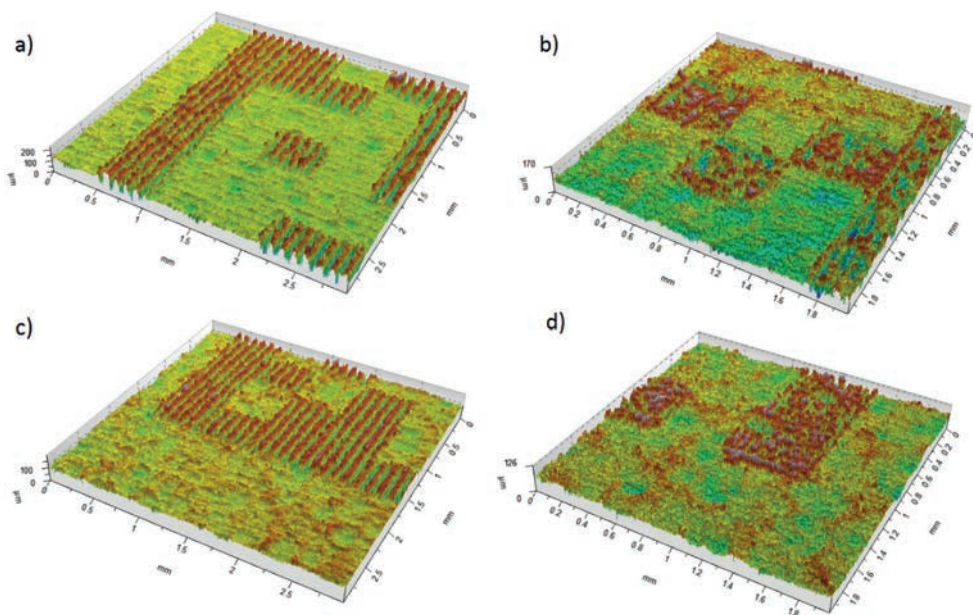


Fig. 14. Printed surface of Data Matrix codes received in the study a) Class A code – 6 stripes in a dark pixel area; b) Class A code – 13 stripes in a dark pixel area; c) Class C code with 6 stripes; d) Class C code with 13 stripes
Source: Authors.

Conclusions

Changes occurring at the surface of markings are responsible for code quality loss. The method of printing dark pixels with 13 deep stripes provided a marking with better durability than that with 6 stripes. In the former method, roughness patterns were less prone to mechanical damage and more resistant to chrome rinse. The surface had a more favourable (convex) Abbot curve - smaller values of functional value parameters. Roughness height parameters ensure high code contrast (diffraction can proceed on dark pixels).

Surface marking should best be conducted with lasers that can modulate energy density, depending on the printed fragment of a code. High energy over a large area is necessary to smooth initial roughness peaks in dark pixel areas and to remove initial roughness. High energy density is also necessary to reduce the level of contrasting bright pixel areas. Energy density should be maintained or reduced while printing diffraction stripes on dark pixel areas – Fig. 15.

Surfaces produced in this way will have a convex Abbot curve with a small peak material volume V_{mp} . Their removal in successive technological operations will not result in the loss of code contrast (SC) and modulation (MOD).

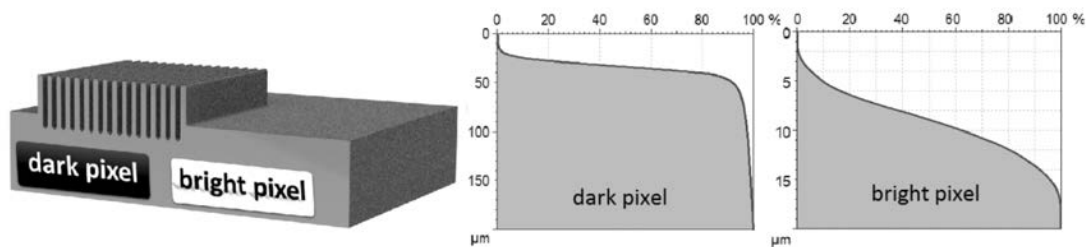


Fig. 15. Abbott curves for an idealised surface fragment of a 2D Data Matrix code laser-printed on metallic surface

Source: Authors.

To maintain high contrast, printed stripes should constitute a substantial part of surface volume - high V_v and V_{vv} parameters. In each case, their depth and number should fit the type of used material, code, and pixel size.

General guidelines were formulated based on investigations conducted on aluminium parts. However, due to the aggressive character of other types of electrolyte treatment, our guidelines should be valid for permanent marking with different code types of parts made from other non-ferrous metals or steel.

References

1. The Global Language of Business. GS1 General Specifications – The foundational GS1 standard that defines how identification keys, data attributes and barcodes must be used in business applications. www.gs1.org release 16.0, ratified, Jan 2016.
2. The Global Language of Business. GS1 DataMatrix Guideline – Overview and technical introduction to the use of GS1 DataMatrix. www.gs1.org release 2.2.1, ratified, July 2015.
3. ISO/IEC 18004:2015, Information technology. Automatic identification and data capture techniques. QR Code bar code symbology specification.
4. The Global Language of Business. GS1 2D Barcode Verification Process Implementation Guideline – developed with the intention of providing a clear explanation on the practical implications of 2D Barcode Verification within the GS1 System. www.gs1.org release 1.3.21, ratified, Jul 2015.
5. Shin D-H., Jung J., Chang B-H.: “The psychology behind QR codes: User experience perspective”. *Comp in human Behav.* vol 28 2012, pp. 1417–1426, <http://dx.doi.org/10.1016/j.chb.2012.03.004>.
6. Fino E.R., Martin-Gutierrez J., Meneses Fernandez M.D., Armas Davara E.: “Interactive Tourist Guide: Connecting Web 2.0, Augmented Reality and QR Codes”. *Procedia Comp. Science* vol. 25 2013, pp. 338–344. doi: 10.1016/j.procs.2013.11.040.
7. Lorenzi D., Vaidya J., Chun S., Shafiq B., Atluri V.: “Enhancing the government service experience through QR codes on mobile platforms”. *Government Inf. Quart.* vol. 31 2014, pp. 6–16, <http://dx.doi.org/10.1016/j.giq.2013.05.025>

8. Barrera J.F., Mira-Agudelo A., Torroba R.: "Experimental QR code optical encryption noise-free data recovering". *Optics Letters*, vol. 39, no. 10, 2014. <http://dx.doi.org/10.1364/OL.39.003074>.
9. Qin Y., Gong Q.: "Optical information encryption based on incoherent superposition with the help of the QR code". *Opt. Comm.*, vol. 310 2014, pp. 69–74. <http://dx.doi.org/10.1016/j.optcom.2013.07.062>.
10. Ramya S., Sheeba Joice C.: "An Optimized Image and Data Embedding in Color QR Code". *Middle-East Jour. of Scien. Research*, vol. 23 2015, pp. 66–72. DOI: 10.5829/idosi.mejsr.2015.23.ssps.15.
11. Jangsombatsiri W., Porter J.D.: "Laser Direct-Part Marking of Data Matrix Symbols on Carbon Steel Substrates". *J. Manuf. Sci. Eng* vol. 129(3) 2007, pp. 583–591. doi:10.1115/1.2716704.
12. Harrison P.W., Patent No. US 6075223, "High contrast surface marking". Thermark LLC, Pittsburgh Pa. 2000.